

a possible "active" process, could be postulated, it appears more reasonable to be critical of the assumption of rate-determining drug diffusion into the biophase.

An alternate explanation may be that drug action, as manifested by the degree of inhibition of generation rate, increases the sensitivity of the organism to further drug action until the steady-state generation rate is achieved. This "feedback" phenomenon is explainable on the premise that the rapidly equilibrated drug concentration in the biophase is competitive for receptor sites with a metabolic intermediate produced by the growing organism.

An analogy can be drawn to the sulfonamide-*p*-aminobenzoic acid competition. The initial fraction of receptor sites that is drug-receptor complex is reflected by an initial decrease in generation rate. This results in a diminution of the production of a vital metabolic intermediate. Subsequent depletion of excess stores of this intermediate in the normal metabolic or generation processes of the organism results in less amounts to compete with drug concentrations in the biophase, greater fractions of drug-receptor complex, and, consequently, further slowing of generation rates. On dilution of the drug with fresh medium, the drug in the organism's biophase rapidly reequilibrates with the consequence of less drug-bound receptor sites. A new steady-state production of metabolic intermediate may occur. This results in the observed reasonably rapid increase in microbial generation to new steady-state conditions (Fig. 2). A kinetically equivalent phenomenon is that the feedback is mediated by decreasing the number of available receptor sites concomitant with decreasing growth rates.

REFERENCES

(1) C. Lewis and H. W. Clapp, *Antibiot. Chemother.*, **11**, 118 (1961).

(2) J. Davies, P. Anderson, and B. D. Davis, *Science*, **149**, 1096(1965).

(3) E. R. Garrett, *Arzneim. Forsch.*, **16**, 1364(1966).

(4) E. R. Garrett and G. H. Miller, *J. Pharm. Sci.*, **54**, 427 (1965).

(5) J. B. Mielck and E. R. Garrett, *Chemotherapy*, **14**, 337 (1969).

(6) E. R. Garrett and O. K. Wright, *J. Pharm. Sci.*, **56**, 1576 (1967).

(7) E. R. Garrett, G. H. Miller, M. R. W. Brown, and K. Smith, *J. Med. Chem.*, **9**, 203(1966).

(8) E. R. Garrett, J. B. Mielck, J. K. Seydel, and H. J. Kessler, *ibid.*, **12**, 740(1969).

(9) E. R. Garrett, G. H. Miller, and M. R. W. Brown, *J. Pharm. Sci.*, **55**, 593(1966).

(10) E. R. Garrett and M. R. W. Brown, *J. Pharm. Pharmacol.*, **15**, 185(1963).

(11) E. R. Garrett, *Arzneim. Forsch.*, **17**, 795(1967).

ACKNOWLEDGMENTS AND ADDRESSES

Received October 3, 1969, from the *College of Pharmacy, J. Hillis Miller Health Center, University of Florida, Gainesville, FL 32601*

Accepted for publication January 2, 1970.

The authors thank Dr. George B. Whitfield, Manager, Infectious Diseases Research, The Upjohn Co., Kalamazoo, Mich., for the supplies of spectinomycin, and Mr. George L. Perry, Sr., for technical assistance.

* To whom communications regarding this paper should be addressed.

Pharmacokinetic Evidence for Saturable Renal Tubular Reabsorption of Riboflavin

WILLIAM J. JUSKO and GERHARD LEVY*

Abstract □ Pharmacokinetic relationships have been developed to characterize a multicompartment drug distribution and elimination model which includes a saturable renal tubular reabsorption process. The derived expressions have been applied to serum concentration and urinary excretion data obtained after rapid intravenous administration of riboflavin to man and dog. The mathematical relationships and experimental data demonstrate the dependence of renal clearance on the serum concentration of the drug and on urine flow rate. The results of this study indicate that the renal excretion of riboflavin, like that of several other water-soluble vitamins, involves saturable tubular reabsorption as well as tubular secretion.

Keyphrases □ Riboflavin—saturable renal tubular reabsorption □ Renal tubular reabsorption, secretion—riboflavin □ Flavin—inulin—clearance ratio □ Pharmacokinetics—riboflavin renal clearance

A number of natural substances are known to be reabsorbed from renal tubules by a saturable process. Among these are the water-soluble vitamins: thiamine (1), pantothenic acid (2), and ascorbic acid (3). The renal excretion of another water-soluble vitamin, riboflavin, has been shown (4) to involve tubular secretion in man, and it has recently been suggested (5) that tubular reabsorption of riboflavin occurs in the chicken. In addition,

an analysis of published data (6) indicates that the renal clearance of riboflavin in man decreases at lower serum levels of the vitamin.

A substance that undergoes saturable renal tubular reabsorption will characteristically yield higher renal clearances with increasing serum concentrations (7). The kinetics of this process have not been studied in detail, particularly over a wide concentration range such as is obtained after rapid intravenous injection of the substance. The single-injection technique for the study of renal clearance is often considered unsuitable (7) because of the difficulty of characterizing and accounting for the effect of rapid flux of the drug between plasma and tissue. Thus, this technically simpler method is often rejected in favor of the commonly used constant intravenous infusion method where plasma and tissue levels of the drug are maintained relatively constant. However, the constant infusion method will not reveal a possible concentration dependence of renal clearance unless the study is carried out at several, widely different infusion rates.

The purpose of this report is to present mathematical relationships which may be utilized for pharmacokinetic

characterization, after rapid intravenous injection, of a multiple-compartment model which includes a saturable renal tubular reabsorption process. The derived expressions will be applied to serum concentration and urinary excretion data obtained after rapid intravenous administration of riboflavin to man and dog.

THEORETICAL

Renal Clearance Expressions—A multicompartment model in which drug is administered by single injection into the central compartment (which includes plasma) is depicted in Fig. 1. The distribution of drug between the central compartment (Subscript 1) and the tissue compartment (Subscript 2) is characterized by the apparent first-order transfer rate constants k_{12} and k_{21} . The entry of drug into the renal tubules is assumed to be by a first-order process characterized by the rate constant k_e . This may involve glomerular filtration with or without a tubular secretion component, provided the secretion process is of such high capacity as not to be saturated under the experimental conditions. The tubular reabsorption of the compound (transfer from urine to plasma) is considered to be of relatively low capacity (saturable) so that the Michaelis-Menten parameters T_m (maximum transport capacity) and K_m (Michaelis-Menten constant) are applicable. An extrarenal elimination component, represented by the apparent first-order rate constant k_{13} , is also employed. The renal clearance expressions to be derived are applicable to the described renal excretion mechanisms even if the extrarenal components of the model are more or less complex than those presented here.

The differential equation for the rate of urinary excretion (dX_u/dt) is

$$\frac{dX_u}{dt} = k_e \cdot X_1 - \frac{T_m \cdot C_u}{K_m + C_u} \quad (\text{Eq. 1})$$

where C_u is the concentration of drug in the urine. This is assumed to reflect the concentration of drug at the site of tubular reabsorption. Since

$$X_1 = C_p \cdot V_c \quad (\text{Eq. 2})$$

and

$$k_e = Cl_f/V_c \quad (\text{Eq. 3})$$

therefore,

$$Cl_f \cdot C_p = k_e \cdot X_1 \quad (\text{Eq. 4})$$

where C_p is the plasma concentration of drug, V_c is the volume of the central compartment, and Cl_f is the clearance for drug transfer from plasma to urine. Substituting Eq. 4 into Eq. 1 yields

$$\frac{dX_u}{dt} = Cl_f \cdot C_p - \frac{T_m \cdot C_u}{K_m + C_u} \quad (\text{Eq. 5})$$

Upon dividing both sides of Eq. 5 by C_p , the net or observed renal clearance (Cl_T) is described by

$$Cl_T = Cl_f - \frac{T_m \cdot C_u}{C_p(K_m + C_u)} \quad (\text{Eq. 6})$$

Equation 6 depicts the typical dependence of net clearance on plasma concentration of a drug subject to saturable tubular reabsorption. At relatively high C_p values, the last term of the equation becomes insignificant and $Cl_T \approx Cl_f$, which provides a method of estimating Cl_f .

Equation 6 can be further rearranged to yield

$$C_u = T_m \cdot \frac{C_u}{C_p(Cl_f - Cl_T)} - K_m \quad (\text{Eq. 7})$$

which, with a known Cl_f value, permits a linearization of experimental data whereby T_m and K_m can be determined from the slope and intercept, respectively, of a plot of C_u versus $C_u/C_p(Cl_f - Cl_T)$.

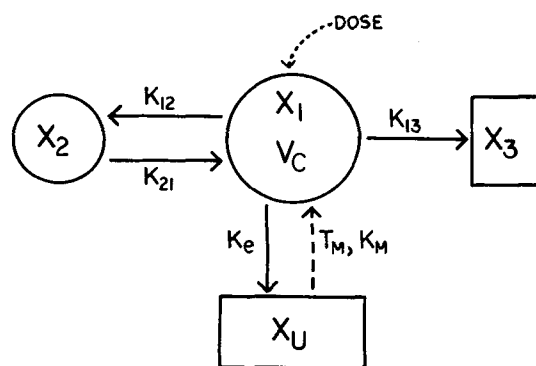


Figure 1—Multiple-compartment open model with central (X_1, V_c), tissue (X_2), urine (X_u), and extrarenal (X_3) compartments. Symbols next to the arrows represent transfer rate constants between compartments. Apparent volume and amounts of drug are designated by V_c and X , respectively.

Effect of Urine Flow Rate—At relatively high urine concentrations of drug (where $C_u \gg K_m$), Eq. 6 reduces to

$$Cl_T = Cl_f - \frac{T_m}{C_p} \quad (\text{Eq. 8})$$

At relatively low urine concentrations of drug (where $K_m \gg C_u$), Eq. 6 reduces to

$$Cl_T = Cl_f - \frac{C_u \cdot T_m}{C_p \cdot K_m} \quad (\text{Eq. 9})$$

Since

$$\frac{C_u}{C_p} = \frac{Cl_T}{R} \quad (\text{Eq. 10})$$

where R is the urine flow rate, Eq. 9 may be written as

$$Cl_T = Cl_f - \frac{Cl_T \cdot T_m}{R \cdot K_m} \quad (\text{Eq. 11})$$

Equation 8 shows that the net renal clearance (Cl_T) is independent of urine concentration (C_u) at relatively high urine and serum concentrations of drug. Consequently, Cl_T is also independent of urine flow rate under these conditions. On the other hand, Cl_T increases with increasing urine flow rate (R) at low plasma and urine concentrations (Eq. 11). Thus, evaluation of the effect of urine flow on renal clearances will provide further evidence for a saturable renal tubular reabsorption mechanism.

Explicit Solution for Transfer Rate Constants—The remaining differential equations that describe the multicompartment model shown in Fig. 1 are:

$$\frac{dX_1}{dt} = -k_e \cdot X_1 + \frac{T_m \cdot C_u}{K_m + C_u} - k_{12} \cdot X_1 - k_{13} \cdot X_1 + k_{21} \cdot X_2 \quad (\text{Eq. 12})$$

$$\frac{dX_2}{dt} = k_{12} \cdot X_1 - k_{21} \cdot X_2 \quad (\text{Eq. 13})$$

$$\frac{dX_3}{dt} = k_{13} \cdot X_1 \quad (\text{Eq. 14})$$

where the k 's are apparent first-order rate constants dictating the rate of change (dX/dt) in the amounts of drug (X) in the respective compartments.

Equation 2 can be substituted into Eq. 14 to yield

$$\frac{dX_3}{dt} = k_{13} \cdot V_c \cdot C_p \quad (\text{Eq. 15})$$

The volume of the central compartment, V_c , can be determined after single i.v. injection of a drug from

$$V_c = \text{dose}/C_p^0 \quad (\text{Eq. 16})$$

where C_p^0 is the zero-time plasma drug concentration obtained by nonlinear least-squares extrapolation. At time = infinity (∞), X_3^∞ is the difference between the dose of drug administered and the total urinary recovery of the drug. Since

$$X_3^\infty = \int_0^\infty \frac{dX_3}{dt} \cdot dt \quad (\text{Eq. 17})$$

then by substituting from Eq. 15:

$$X_3^\infty = k_{13} \cdot V_c \cdot \int_0^\infty C_p \cdot dt \quad (\text{Eq. 18})$$

of which the integral portion is the area under the plasma level curve (AUC) which can be readily determined. Thus, k_{13} can be calculated from

$$k_{13} = X_3^\infty / V_c \cdot (\text{AUC}) \quad (\text{Eq. 19})$$

Similarly, X_3 as a function of time is

$$X_3^t = k_{13} \cdot V_c \cdot \int_0^t C_p \cdot dt \quad (\text{Eq. 20})$$

Substituting Eqs. 1 and 2 into Eq. 12 yields

$$\frac{dC_p}{dt} \cdot V_c = -\frac{dX_u}{dt} - k_{12} \cdot X_1 - k_{13} \cdot C_p \cdot V_c + k_{21} \cdot X_2 \quad (\text{Eq. 21})$$

which, upon rearrangement, becomes

$$\frac{dC_p}{dt} \cdot V_c + \frac{dX_u}{dt} + k_{13} \cdot C_p \cdot V_c = -k_{12} \cdot X_1 + k_{21} \cdot X_2 \quad (\text{Eq. 22})$$

As evident from Eq. 13, both sides of Eq. 22 are equal to $-dX_2/dt$, or

$$\frac{dX_2}{dt} = -\frac{dC_p}{dt} \cdot V_c - \frac{dX_u}{dt} - k_{13} \cdot C_p \cdot V_c \quad (\text{Eq. 23})$$

All parameters on the right-hand side of Eq. 23 can be determined directly from experimental data and from Eqs. 16 and 19. Thus, successive values of dX_2/dt as a function of time can be calculated. Since

$$X_2^t = \int_0^t \frac{dX_2}{dt} \cdot dt \quad (\text{Eq. 24})$$

values of X_2 as a function of time can be calculated using computer numerical integration¹ of Eqs. 23 and 24. With values of X_2 , dX_2/dt , and X_1 thus obtainable at successive times (Eqs. 24, 23, and 2, respectively), rearrangement of Eq. 13 provides a slope-intercept method for determining the transfer rate constants k_{12} and k_{21} since

$$\frac{dX_2/dt}{X_1} = k_{12} - k_{21} \cdot \frac{X_2}{X_1} \quad (\text{Eq. 25})$$

Calculation of the amounts of drug in the respective compartments of the model as a function of time can then be achieved by use of Eqs. 2 (for X_1), 24 (for X_2), and 20 (for X_3). X_u as a function of time can be determined directly from the urinary excretion data.

EXPERIMENTAL

The studies were carried out in a healthy male human subject (26 years, 85.4 kg.) and an apparently healthy female mongrel dog (29.5 kg.). The human subject received an intravenous dose of 31 mg. riboflavin (FR) as sodium riboflavin-5'-phosphate (FMN).² Urine was collected at appropriate intervals for a total of 48 hr.

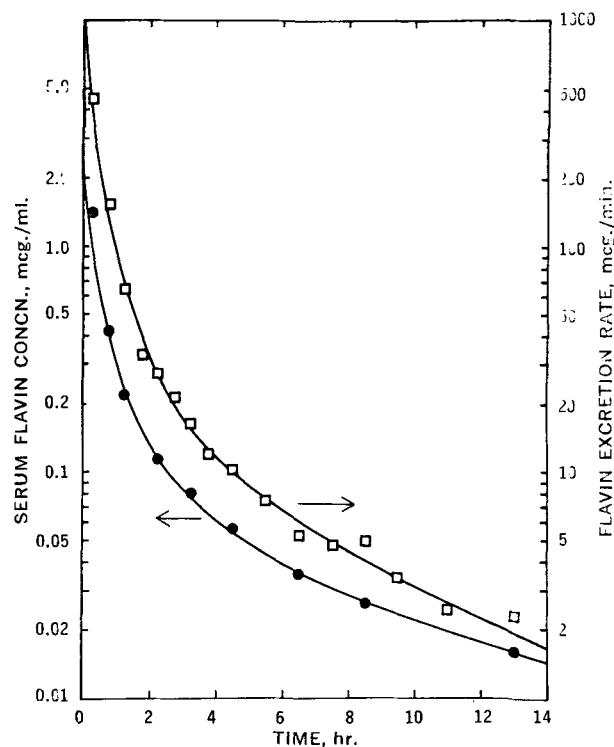


Figure 2—Serum concentrations (●) and urinary excretion rates (□) of total riboflavin in a human subject after rapid intravenous injection of 31 mg. riboflavin (FR) as riboflavin-5'-phosphate (FMN). Solid lines represent a least-squares triexponential computer fit of the data.

Blood samples (16 ml. each) were obtained from the antecubital vein at -0.5, 0.25, 0.75, 1.25, 2.25, 3.25, 4.5, 6.5, 8.5, 13.0, and 25.0 hr. after FMN injection. These were midtimes of urine-collection periods. The serum and urine samples were analyzed for FR, FMN, and endogenous creatinine.

Dog Study³—The dog was fasted overnight prior to the experiment but was allowed free access to water. Anesthesia was induced with sodium pentobarbital,⁴ 30 mg./kg., and was maintained for the duration of the experiment by administration of 2-4 mg./kg. of the anesthetic approximately every hour as needed.

The animal was prepared for study using standard surgical techniques with care being taken to minimize blood loss. A tracheal cannula was inserted to prevent obstruction of respiration. A venous cannula in the left foreleg was used for infusion of isotonic saline solution to maintain adequate hydration of the dog. A 300-mg. priming dose of inulin⁵ was injected intravenously 30 min. prior to rapid intravenous administration of 18.3 mg. of riboflavin.⁶ Using a cannula placed in a right foreleg vein, inulin solution (12 mg./ml., 2 ml./min.) was infused for the duration of the experiment. Urine was generally collected every 10 min. for 280 min. from cannulas placed in each ureter. Arterial blood samples (11 ml. each) were collected at the midtimes of the urine-collection periods by means of a cannula placed into a left hindleg artery of the dog. Dilute heparin solution (50 units/ml.) was maintained in the arterial cannula between collection times to prevent clotting of blood in the cannula.

Analytical Methods—Riboflavin and FMN in serum and urine were assayed fluorometrically as described previously (9). Inulin and endogenous creatinine were determined by standard colorimetric techniques (10). There was no interference in the assay of any of the compounds due to the presence of the others.

Data for flavins and inulin were corrected for blank readings of urine and serum obtained prior to administration of the compounds to the test subjects.

¹ Mathematically, this can be done using either the trapezoidal rule or Simpson's rule (8).

² Sodium riboflavin-5'-phosphate, Hoffmann-La Roche, Nutley, N. J.

³ The authors gratefully acknowledge the help of Dr. Barbara R. Rennick in this experiment.

⁴ Diabulal, 60 mg./ml., Diamond Laboratories, Des Moines, Iowa.

⁵ Inulin, Nutritional Biochemicals Corp., Cleveland, Ohio.

⁶ Riboflavin USP, Hoffmann-La Roche, Nutley, N. J.

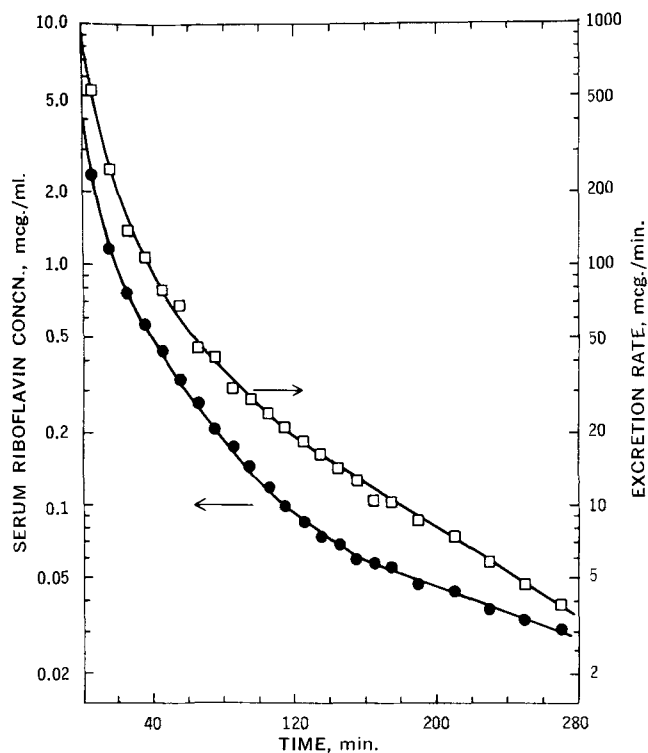


Figure 3—Serum concentrations and urinary excretion rates of riboflavin in a dog after rapid intravenous injection of 18.3 mg. riboflavin. Symbols and lines are defined as in Fig. 2.

RESULTS

Renal Clearances—The declines in serum concentrations and urinary excretion rates of flavin after rapid intravenous injection of the vitamin to the man and the dog are shown in Figs. 2 and 3, respectively. The data are plotted semilogarithmically as a function of time. Graphical analysis of the experimental results by the method of residuals (11) indicated that the decline of all data was triexponential. A nonlinear least-squares computer fit⁷ of the data was obtained using the "NLIN" digital computer program of

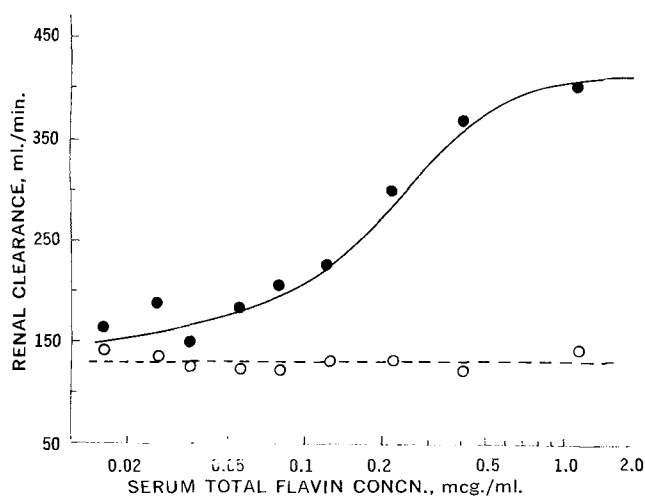


Figure 4—Renal clearances of total riboflavin (●) in the human subject as a function of serum total riboflavin concentration. Solid line represents a least-squares fit of the data according to the constants of Table I. Open symbols show simultaneously obtained creatinine clearances.

⁷ The contribution of C.D.C. 6400 computer time by the State University of New York at Buffalo Computer Center is gratefully acknowledged.

Table I—Pharmacokinetic Constants^a Describing the Serum Concentrations and Urinary Excretion Rates of Riboflavin after Its Intravenous Administration to Man and Dog

| Constant ^b | Serum Concentrations | | Urinary Excretion Rates | |
|------------------------------|----------------------|--------|-------------------------|-------|
| | Man | Dog | Man | Dog |
| A, mcg./J | 1.83 | 2.40 | 803 | 594 |
| α , hr. ⁻¹ | 3.24 | 10.4 | 3.02 | 9.69 |
| B, mcg./J | 0.316 | 1.43 | 94.7 | 257 |
| β , hr. ⁻¹ | 0.717 | 1.86 | 0.824 | 2.46 |
| C, mcg./J | 0.0719 | 0.0975 | 14.6 | 58.1 |
| γ , hr. ⁻¹ | 0.120 | 0.258 | 0.148 | 0.602 |

^a From least-squares computer fits of Eq. 26. ^b For serum: J = ml.; for urinary excretion: J = min.

Marquardt (12). The general equation which was fit to the data is

$$F = A \cdot e^{-\alpha t} + B \cdot e^{-\beta t} + C \cdot e^{-\gamma t} \quad (\text{Eq. 26})$$

where F represents either flavin plasma levels or urinary excretion rates, t is time, and the remaining symbols are constants. Since the experimental data extended over a range of more than two orders of magnitude, they were converted to their respective logarithm values to reduce bias resulting from the numerical size of the larger values relative to the smaller values. The six parameters which were obtained for each of the four sets of data are shown in Table I; the solid lines of Figs. 2 and 3 represent the computer least-squares fit to the respective data.

All human pharmacokinetic analyses in this study were carried out on the basis of total flavin levels, *i.e.*, riboflavin and riboflavin-5'-phosphate (FMN). This was necessary because of the rapid dephosphorylation of FMN in the blood *in vitro* (13) and because of limited assay sensitivity for FMN in the presence of an excess of riboflavin. However, estimations of renal clearances of FMN during the early sampling periods (when FMN levels were high) showed that the clearance of this substance was similar to that of riboflavin itself.

The renal clearances of flavin in man are shown in Fig. 4 plotted as a function of serum flavin concentration. All renal clearance values were obtained by the usual method of dividing the urinary excretion rate by the midtime serum concentration. The solid line of Fig. 4 represents flavin clearances calculated from the least-squares parameters of Table I. The figure also shows the endogenous creatinine clearances obtained at the same times as a measure of the glomerular filtration rate (GFR). The GFR remained essentially constant for the duration of the experiment, and the average value obtained was 130 ml./min.

The flavin clearances in Fig. 4 show a profile characteristic of saturable tubular reabsorption since the net clearance values progressively diminish as serum levels of the vitamin decline. Tubular secretion of the vitamin also occurs since the net clearance exceeds the GFR. Since the substrate concentration of the tubular secretory process (presumably plasma or cell water concentration of flavin) is appreciably lower than the flavin concentration in the urine, and since the net clearance of flavin increases rather than decreases at

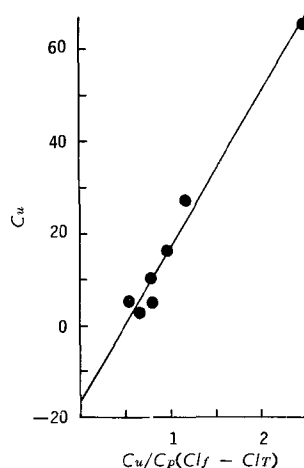


Figure 5—Linearization method for obtaining the Michaelis-Menten constants of the renal tubular reabsorption process according to Eq. 7. The line fitted to the data has a slope of T_m and an intercept of $-K_m$.

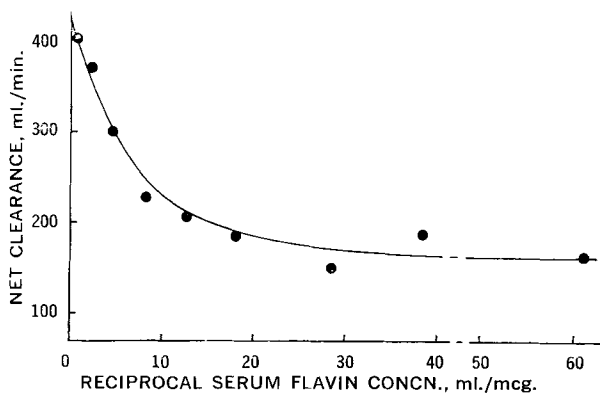


Figure 6—Net renal clearance (Cl_T) of riboflavin in man plotted as a function of reciprocal serum concentration. Symbols are experimental data, and the line represents clearances calculated according to Eq. 6 using the derived values of Cl_f , T_m , and K_m .

high plasma concentrations of the vitamin, it was assumed that the secretory process was not capacity limited under the experimental conditions. Tubular secretion and glomerular filtration of flavin were therefore treated pharmacokinetically as apparent first-order processes. On the assumption that the contribution of the tubular reabsorption process to the net clearance is negligible at relatively high serum concentrations of the vitamin, a theoretical Cl_f was calculated from the C_p^0 and dX_u/dt values obtained by computer from plots of these data as a function of time.

This value, 420 ml./min. in man, was taken as an estimate of Cl_f and used in Eq. 7 for linearization of the renal excretion data by a plot of C_u versus $C_p \cdot (Cl_f - Cl_T)$. The graphical results are shown in Fig. 5. A least-squares fit of the data yielded a slope of 33.3 mcg./min. for T_m and an intercept K_m value of 16.3 mcg./ml. The three renal excretion parameters can be more readily obtained using Eq. 6 with a plot such as shown in Fig. 6. A direct computer fit of Eq. 6 to the experimental data using the Marquardt digital computer program (12) yielded nearly identical values for Cl_f , T_m , and K_m (425 ml./min., 34.1 mcg./min., and 17.9 mcg./ml., respectively). In the human subject, the urine flow rates were essentially constant at about 1 ml./min. The curve shown in Fig. 6 represents the calculated net clearance (Cl_T) of flavin, using the graphically derived values of Cl_f , T_m , and K_m in Eq. 6. The excellent fit of the experimental points to the calculated line demonstrates the suitability of the pharmacokinetic expressions for describing the concentration dependence of the renal clearances of riboflavin.

The renal clearances of riboflavin and urine flow rates obtained in the dog are shown in Fig. 7 as a function of time. The solid line depicts renal clearance values calculated from the least-squares parameters for the dog listed in Table I. The inulin clearances which were obtained as a measure of GFR were relatively constant and averaged 98.0 ml./min. with a standard deviation of 7.6. The fact that the flavin-inulin clearance ratio is greater than unity and the

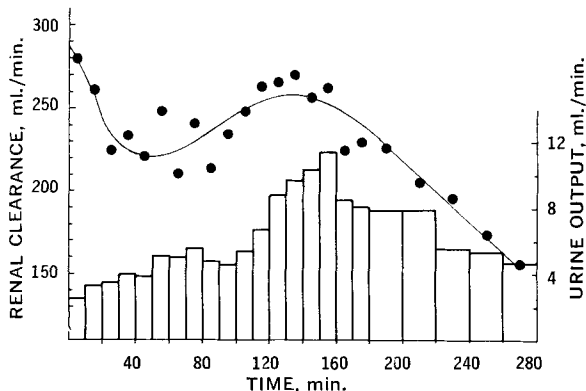


Figure 7—Renal clearance of riboflavin (●) and urine flow rates (bars) in the dog as a function of time after riboflavin injection. The solid curve is a computer least-squares fit of the renal clearance data according to the constants of Table I.

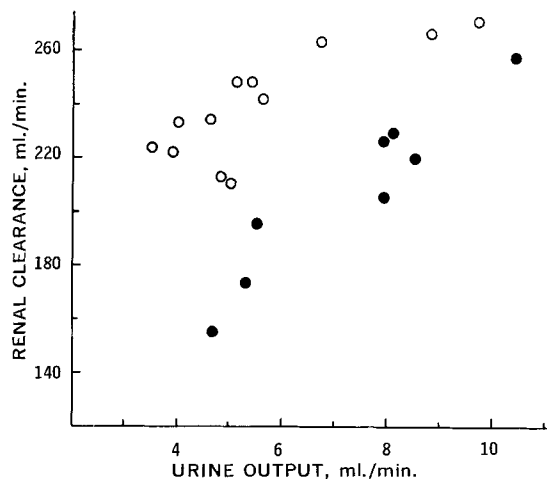


Figure 8—Effect of urine flow rate on riboflavin clearance in the dog. Open symbols are results obtained during 0–140 min. and solid symbols are results obtained during 140–280 min. after riboflavin administration.

decrease in the clearance values of riboflavin with decreasing serum concentrations indicate that the renal clearance of riboflavin in the dog, as in man, involves both tubular secretion and saturable tubular reabsorption. These data also demonstrate the dependence of net renal clearance on urine flow rate, but the relationship is better exemplified in Fig. 8. In that figure, the net renal clearance of riboflavin is plotted as a function of urine flow rate with the data obtained in the first 140 min. separated from the data subsequently obtained. As predicted by Eq. 5, there is little effect of urine flow on the early riboflavin clearances ($C_p > 0.06$ mcg./ml.), but net clearance increased markedly with increasing urine flow rate when riboflavin serum and urine levels were relatively low.

For the dog, the earlier described computer program (12) was used to calculate Cl_f , T_m , and K_m and values are listed in Table II.

Distribution and Elimination Parameters of the Model—The last portion of the *Theoretical* section includes methods of calculating the rate constants k_{13} , k_{12} , and k_{21} . The volume of the central compartment for man and dog was obtained using Eq. 16, with C_p^0 determined from the least-squares parameters for the serum level data in Table I where

$$C_p^0 = A + B + C \quad (\text{Eq. 27})$$

The areas under the plasma level curves for man and dog were

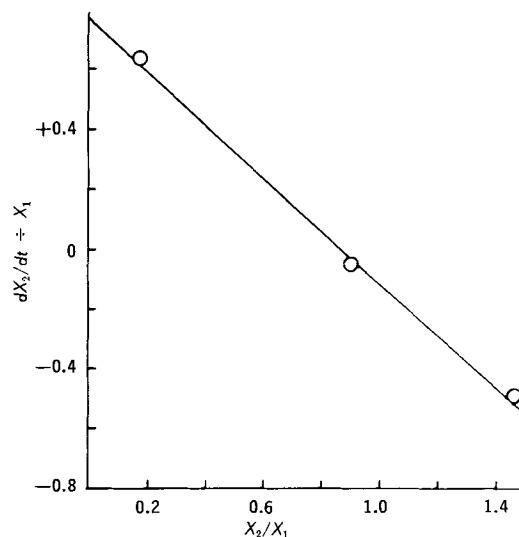


Figure 9—Plot of pharmacokinetic data from the human according to Eq. 25 to yield an intercept of k_{12} on the ordinate and a slope of $-k_{21}$. Circles are values calculated directly from the experimental data and the line is the computer regression calculation.

Table II—Pharmacokinetic Constants of the Multicompartment Model for Riboflavin Distribution and Elimination in Man and Dog

| Constant | Man | Dog |
|------------------------------|-------|-------|
| Cl_f , ml./min. | 420 | 232 |
| T_m , mcg./min. | 33.3 | 21.9 |
| K_m , mcg./ml. | 16.3 | 9.61 |
| k_e , hr. ⁻¹ | 1.80 | 2.98 |
| k_{13} , hr. ⁻¹ | 0.133 | 0.433 |
| k_{12} , hr. ⁻¹ | 0.768 | 3.01 |
| k_{21} , hr. ⁻¹ | 0.872 | 5.11 |
| V_c , l. | 14.0 | 4.66 |
| V_c , % b.w. | 16.4 | 15.8 |
| Wt., kg. | 85.4 | 29.5 |
| Dose, mg. | 31.0 | 18.3 |
| Urinary excretion, % | 89.8 | 85.0 |

found to be 1.62 and 1.36 mcg. hr./ml., respectively. The k_{13} values for man and dog, which were calculated by means of Eq. 19, are 0.133 and 0.433 hr.⁻¹, respectively. All numerical integrations were carried out using the trapezoidal rule with sequential areas determined at 0.05-hr. increments.

Figure 9 shows the plot of $dX_2/dt/X_1$ versus X_2/X_1 for the data obtained in the human subject. There is good agreement between the points calculated directly from the experimental data and the computer-calculated regression line. A similar plot was obtained for the dog; the resultant values of k_{12} and k_{21} which were found in the two experiments are listed in Table II.

Since only one man and one dog were employed in the present study, the rate constants and pharmacokinetic parameters listed in Table II cannot be used as a measure of species differences. However, it is interesting to note several similarities in the data of Table II for man and dog. The volume of the central compartment is about 16% of body weight in both. The percent urinary excretion

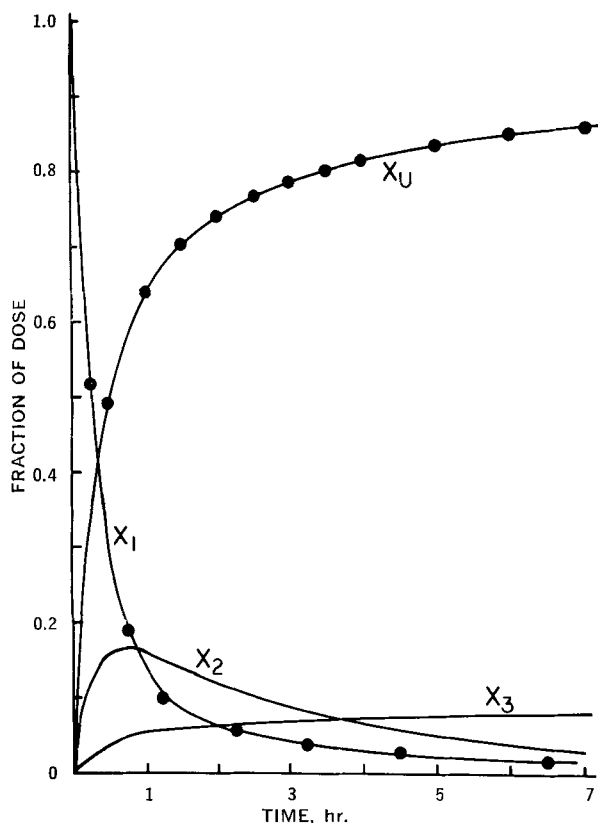


Figure 10—Amounts of total riboflavin (as fraction of the administered dose) as a function of time in the four compartments of the pharmacokinetic model for man. Data points were obtained experimentally from serum concentrations (for Curve X_1) and urinary excretion rates (for Curve X_u).

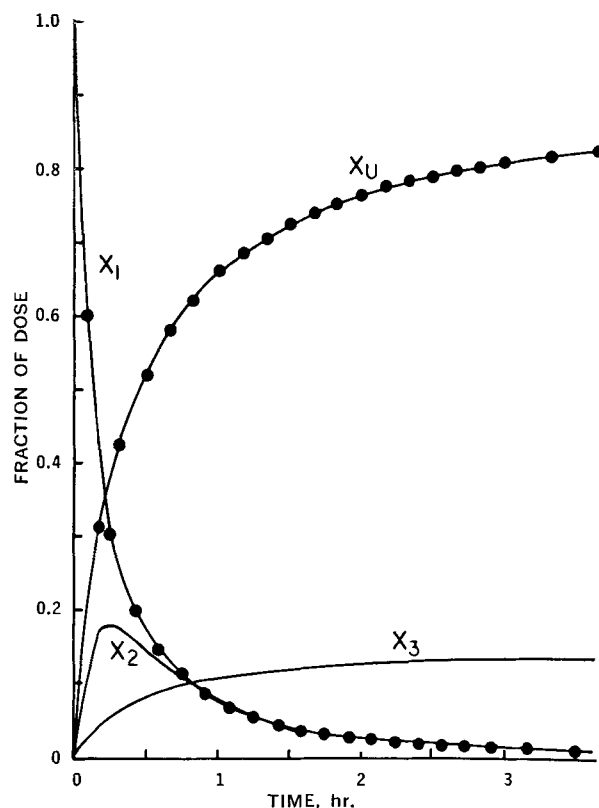


Figure 11—Fraction of the riboflavin dose as a function of time in the four compartments of the pharmacokinetic model for the dog. Data points and lines were obtained as in Fig. 10.

and the ratios of $k_e:k_{13}$, $k_{21}:k_{12}$, and $T_m:K_m$ are similar. However, the tubular secretion process (Cl_f) had a relatively much greater capacity in the dog, resulting in more rapid elimination of the vitamin.

The parameters of Table II were used with the appropriate equations of the *Theoretical* section to calculate the fraction of the dose of flavin in the respective compartments of the pharmacokinetic model of Fig. 1. The results of such calculations are shown in Fig. 10 for the man and in Fig. 11 for the dog. The experimental data shown for the central (X_1) and urine (X_u) compartments are in excellent agreement with the calculated curves. As predicted by the several similarities in the parameters listed in Table II, the time courses of fractional drug levels in man and dog are quite similar, except that all processes occur at a more rapid rate in the dog. The parameters and results of Table II and Figs. 10 and 11 were further confirmed using the "MIMED" digital computer analog simulation program (14) with the appropriate differential equations (Eqs. 2 and 12-14).

Calculation of the sum of the fraction of the dose of drug in the various compartments using the derived parameters of the model provides an indication of the overall error involved in the calculations. The discrepancy between the summation of fractional drug levels and the administered dose ranged between 0 and 2%. Since the calculated X_1 and X_u values agreed very well with the experimental data, most of the error can be attributed to calculation of X_2 and particularly X_3 . This is to be anticipated because of the three components of Eq. 23 which must be calculated from the experimental data and the subsequent necessity of integrating this equation at discrete time increments to obtain X_2 values.

DISCUSSION

A pharmacokinetic model has been developed to characterize the kinetics of renal clearance by simultaneous first-order renal excretion and saturable renal tubular reabsorption after rapid intravenous administration of a drug. This model and the results obtained experimentally demonstrate the dependence of renal clearance on the serum concentration of a drug and the rate of urine flow.

It was assumed in the calculations that the urine concentration of drug approximates the concentration at the site of renal tubular reabsorption. If tubular reabsorption occurs in the distal renal tubule, this assumption is probably quite reasonable. The simultaneous occurrence of glomerular filtration, tubular secretion, tubular reabsorption, and water reabsorption produces a proximal to distal gradient in tubular concentrations of drug, and the actual drug concentration at the site of reabsorption will lie between the glomerular filtrate concentration ($\approx C_p$) and the urine concentration in the ureter (C_u). If the actual drug concentration (S) at the site of tubular reabsorption is considered to be the average of the filtrate and urine concentrations,

$$S = \frac{1}{2}(C_p + C_u) \quad (\text{Eq. 28})$$

and since $C_u \gg C_p$, then $S \approx \frac{1}{2}C_u$. Substituting this average concentration into Eq. 6 and rearranging yield

$$Cl_T = Cl_f - \frac{T_m \cdot C_u}{C_p(\frac{1}{2}K_m + C_u)} \quad (\text{Eq. 29})$$

The T_m value, but not the value of K_m , is independent of the assumption represented by Eq. 28. Equation 29 indicates that K_m is simply a proportionality constant which is dependent on the assumption of how best to approximate the drug concentration at the site of reabsorption. It, therefore, should not be used for comparison of data for drugs which are reabsorbed at different sites in the renal tubule.

The renal clearance equations which were developed are independent of the complexity of the extrarenal portion of the model. Drug levels are measured in the serum and urine, and the clearance equations are only concerned with the relationship between the two compartments as reflected by these fluids.

The nonlinear relationship which characterizes the tubular reabsorption mechanism does not permit solution of the extrarenal parameters of the model by use of the usual pharmacokinetic treatments such as described by Rescigno and Segre (15). However, because drug levels were simultaneously determined in two compartments (central and urine), it was possible to develop explicit solutions for the rate parameters k_{13} , k_{12} , and k_{21} . The results of such calculations yield a very good fit to the test data, but the values obtained for X_2 as a function of time may be slightly in error. This error arises from experimental variation in the values of dC_p/dt , dX_u/dt , and C_p ; the necessity of predetermining V_c and k_{13} for use in Eq. 23; and the probable error due to integrating this equation at discrete time increments. The use of computer calculations and least-squares data treatments, however, tends to minimize such error. It is easier to utilize the mathematical relationships described here than to resort to the analog computer for an empirical resolution of the parameters. The linearity of a plot such as is shown in Fig. 9 also provides a test to determine whether or not a more complex model (e.g., two-tissue compartments) might be more appropriate.

The serum concentration and urinary excretion rate data in man and dog could be fitted effectively to a triexponential equation. For a linear multiple-compartment model, such data would be indicative of a three-compartment open model; parameters such as those shown in Table I could be directly utilized for solution of the microscopic transfer rate constants (15). However, because of the nonlinear tubular reabsorption process, this approach was not feasible in this study, and the least-squares triexponential fit of the data (Table I and Eq. 26) was used only for a suitable description of the data which facilitated computer numerical analyses for solution of the pharmacokinetic equations listed in the *Theoretical* section.

With regard to the test compound used in the present study, the data indicate that the renal excretion of riboflavin in man and dog involves a specialized secretory process of apparent high capacity as well as an easily saturated tubular reabsorption process. The first conclusion is based on the renal clearance data which show that riboflavin clearances are much greater than the glomerular filtration rate, even without correction of the clearance data for the moderate extent of serum protein binding of the flavins. Previous work has shown that riboflavin and FMN, in the serum concentration range encountered in this study, are about 60% bound to plasma proteins in man (9). The dog exhibits 19% binding of riboflavin to serum proteins (16). In both species, the extent of flavin binding is independent of serum concentration over the range used

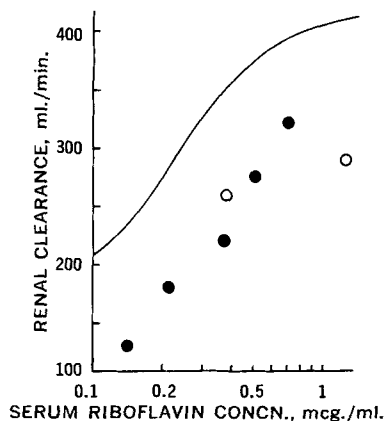


Figure 12—Relationship between renal clearance and serum concentration of riboflavin in a human subject who received 84 mg. riboflavin by intravenous infusion over 2 hr. The open circles are values obtained during the infusion (when serum concentrations were rising) and the solid circles are values obtained postinfusion (when serum concentrations were falling). Based on data from Reference 6. The curve is from Fig. 4 of the present study.

in the present study. It has been further demonstrated that probenecid, a potent inhibitor of many active transport processes (17), inhibits the renal clearance of riboflavin in man (13) and dog (16). Markkanen *et al.* (18) have also shown that probenecid decreases the basal excretion of riboflavin in man and rabbits whose riboflavin intake was limited to that derived from the normal diet. Rennick (19), whose work first demonstrated the tubular secretion of riboflavin in chickens, also noted that this process was inhibited by probenecid.

The decline in renal clearances of riboflavin with decreasing serum levels of the vitamin indicates that the vitamin undergoes saturable tubular reabsorption. The kinetics of this process are well characterized in man and dog by a model which assumes saturable renal tubular reabsorption. Experimental confirmation of the theoretically predicted effect of urine flow rate on the renal clearance of riboflavin in the dog adds further support to this interpretation. Evidence in the literature also suggests a dependence of riboflavin excretion on urine flow rate. Tucker *et al.* (20) and Johnson (21) reported increases in riboflavin excretion in human subjects after diuresis due to increased water intake. A reexamination of data published by Markkanen (22) shows that diuresis induced by acetazolamide and mercaptopimerin also increases the basal excretion of riboflavin in rabbits.

The relationship between renal clearance and serum concentration shown in Fig. 4 was determined under dynamic conditions, *i.e.*, when serum concentrations of riboflavin were changing rapidly. These conditions are quite different from the usual conditions for the determination of clearance values, where relatively constant serum concentrations are maintained by continuous infusion of drug. The question then arises whether the clearance *versus* serum concentration profile obtained in the present study is an artifact due to distribution effects. There is strong evidence that this is not so. First, the magnitude of the clearance changes (almost threefold) is much greater than could be explained by distribution effects, particularly since, according to the pharmacokinetic analysis, no more than 18% of the dose of riboflavin reaches the "tissue" compartment. Second, analysis of riboflavin serum and urinary excretion data from the literature (6) provides independent confirmation of the results of the present study. The renal clearance values calculated from these data, which were obtained by infusing a total of 84 mg. riboflavin over 2 hr., are shown in Fig. 12. The clearance *versus* riboflavin concentration profile is essentially the same as was obtained in the present study, although the numerical values are somewhat lower, probably reflecting differences in body size. The clearance values during infusion of riboflavin (*i.e.*, when the serum concentration of riboflavin was rising) agree well with the postinfusion values (*i.e.*, when the serum concentration of riboflavin was falling). This, and the fact that distribution factors would have much smaller effects when the drug is administered by infusion rather than by rapid intravenous injection, strongly support the conclusions of the present study.

It is now apparent that there exist specialized transport mechanisms for riboflavin, other water-soluble vitamins, and certain amino acids and sugars for renal tubular reabsorption as well as intestinal absorption (3, 7, 23, 24). Both mechanisms are easily saturable. The specialized renal tubular reabsorption process helps to prevent a possible depletion of body levels of these essential nutrients. On the other hand, saturability of transport of nutrients across the small intestine sets an upper limit on the amount of these substances which can be absorbed.

REFERENCES

- (1) H. N. Haugen, *Scand. J. Clin. Lab. Invest.*, **13**, 61(1961).
- (2) K. Roholt and V. Schmidt, *ibid.*, **3**, 108(1951).
- (3) R. F. Pitts, "Physiology of the Kidney and Body Fluids," Yearbook Medical Publishers, Chicago, Ill., 1963, p. 81.
- (4) G. Levy and W. J. Jusko, *J. Pharm. Sci.*, **55**, 1322(1966).
- (5) J. W. Cowan, R. V. Boucher, and E. G. Buss, *Poultry Sci.*, **45**, 538(1966).
- (6) B. Stripp, *Acta Pharmacol. Toxicol.*, **22**, 353(1965).
- (7) H. W. Smith, "The Kidney," Oxford University Press, New York, N. Y., 1951, p. 81.
- (8) M. H. Protter and C. B. Morrey, "College Calculus with Analytic Geometry," Addison-Wesley, Reading, Mass., 1964, p. 524.
- (9) W. J. Jusko and G. Levy, *J. Pharm. Sci.*, **58**, 58(1969).
- (10) "Laboratory Manual of Pediatric Micro- and Ultramicro-Biochemical Techniques," 3rd ed., D. O'Brien and F. A. Ibbott, Eds., Harper and Row, New York, N. Y., 1961, p. 100.
- (11) J. G. Wagner, *Drug Intel.*, **2**, 206(1968).
- (12) D. W. Marquardt, DPE-NLIN, Share General Library Program No. 7-1354, 1964.
- (13) W. J. Jusko, G. Levy, S. J. Yaffe, and R. Gorodischer, *J. Pharm. Sci.*, **59**, 473(1970).

- (14) MIMED, State University of New York at Buffalo Computer Center, adaptation of MIMIC, Control Data Corp., St Paul, Minn., Publ. No. 44610400, 1968.
- (15) A. Rescigno and G. Segre, "Drug and Tracer Kinetics," Blaisdell, Waltham, Mass., 1966, p. 75.
- (16) W. J. Jusko, B. R. Rennick, and G. Levy, to be published.
- (17) K. H. Beyer, H. F. Russo, E. K. Tillson, A. K. Miller, W. F. Verway, and S. R. Gass, *Amer. J. Physiol.*, **166**, 625(1951).
- (18) T. Markkanen, P. Toivanen, A. Toivanen, and E. Sotaniemi, *Scand. J. Clin. Lab. Invest.*, **15**, 511(1963).
- (19) B. R. Rennick, *Proc. Soc. Exp. Biol. Med.*, **103**, 241(1960).
- (20) R. G. Tucker, O. Mickelson, and A. Keys, *J. Nutr.*, **72**, 251(1960).
- (21) R. E. Johnson, *Fed. Proc.*, **5**, 139(1946).
- (22) T. Markkanen, *Z. Vitan. Hormon. Fermentforsch.*, **14**, 72(1965).
- (23) T. H. Wilson, "Intestinal Absorption," Saunders, Philadelphia, Pa., 1962, p. 51.
- (24) W. J. Jusko and G. Levy, *J. Pharm. Sci.*, **56**, 58(1967).

ACKNOWLEDGMENTS AND ADDRESSES

Received September 10, 1969, from the *Department of Pharmaceutics, School of Pharmacy, State University of New York at Buffalo, Buffalo, NY 14214*

Accepted for publication January 12, 1970.

Presented in part to the Basic Pharmaceutics Section, APHA Academy of Pharmaceutical Sciences, Montreal meeting, May 1969.

This investigation was supported in part by Public Health Service Fellowship 5-F1-GM-33,073 for W. J. J. from the National Institutes of General Medical Sciences, Bethesda, Md.

* To whom requests for reprints should be directed.

Distribution, Excretion, and Metabolism of ¹⁴C-Labeled Quaternary Ammonium Salt of Mepazine and Promethazine in Rats

C. L. HUANG, J. A. YEH, and S. Y. HSU

Abstract □ Studies on the biological fate and antimicrobial activity of mepazine and promethazine methiodide are presented. Synthesis of ¹⁴C-methiodide and estimation of the unchanged compound in biological materials are described. After intraperitoneal administration, the majority of these compounds was excreted in feces. The radioactivity in the liver and kidneys prevailed over other organs. Blood levels were low but above the significant level in both compounds. Brain level of promethazine methiodide-¹⁴C was detectable but that of mepazine methiodide-¹⁴C was insignificant. These compounds displayed a significant antimicrobial activity.

Keyphrases □ Mepazine and promethazine ¹⁴C-methiodides—synthesis □ Biological fate—mepazine and promethazine ¹⁴C-methiodides □ UV spectrophotometry—identity □ Paper chromatography—separation □ Radiochromatography—purity determination

Mepazine and promethazine are derivatives of phenothiazine but they display quite a different mode of action. Pharmacologically, mepazine is less potent than chlorpromazine (1-5). The drug possesses a neuroleptic

effect similar to that of chlorpromazine (6-8); however, mepazine is not a drug of choice for the treatment of psychoses because of the high incidences of side effects such as agranulocytosis, seizures, depression of bone marrow, and jaundice. Promethazine (9, 10) finds its use mainly as a potent antihistaminic drug with a prolonged duration of action and as a drug for motion sickness. The difference in the pharmacological activities between these two drugs appears to be attributable to the effect of the side chains attached to the nitrogen of the phenothiazine ring system. All psychoactive phenothiazine derivatives possess a three-carbon bridge between the terminal and the ring nitrogen, while the presence of a two-carbon bridge between the two nitrogens appears to enhance the antihistaminic effect but diminishes the psychoactive properties of phenothiazine derivatives.

Quaternization of a side-chain nitrogen does not seem to decrease the toxicity of phenothiazine neuroleptics (11, 12). In many cases, toxicity appears to be enhanced.